

- (1984); *Brain Res.* **363**, 376 (1986).
8. M. D. Mauk, J. E. Steinmetz, R. F. Thompson, *Proc. Natl. Acad. Sci. U.S.A.* **83**, 5349 (1986).
 9. D. A. McCormick, J. E. Steinmetz, R. F. Thompson, *Brain Res.* **359**, 120 (1985).
 10. T. J. Voneida, D. Christie, R. Bogdanski, B. Chopko, *J. Neurosci.* **10**, 3583 (1990).
 11. C. H. Yeo, M. J. Hardiman, M. Glickstein, *Exp. Brain Res.* **63**, 81 (1986).
 12. L. L. Sears, and J. E. Steinmetz, *Brain Res.* **545**, 114 (1991).
 13. G. Hesslow and M. Ivarsson, *Exp. Brain Res.* **110**, 36 (1996).
 14. Purkinje cells are the sole output neurons of the cerebellar cortex that project to cerebellar deep nuclei (such as the interpositus nucleus) [M. Ito, *The Cerebellum and Neural Control* (Raven Press, New York, 1985)], and these neurons demonstrate synaptic plasticity (for example, long-term depression) hypothesized to be involved in eyeblink conditioning (5).
 15. A circular craniotomy (6 mm diameter) was performed over the left cerebellum, centered over Larsell's HVI (4.5 mm lateral and 1.0 mm rostral to the lambda skull suture). A stainless steel recording base for a hydraulic microdrive (Kopf 650) was cemented over the craniotomy with dental acrylic and stainless steel skull screws. Electrode penetrations could be precisely located anywhere within the 6-mm opening. All surgeries were performed under ketamine HCl (60 mg per kilogram body weight), xylazine (6 mg/kg), and 1 to 2% halothane gas anesthesia. Rabbits ($n = 14$) received 7 days of post-operative recovery.
 16. For recording, a single-unit electrode (Z 64 5 megohm at 1 kHz) was lowered to the surface of the cerebellum and then further lowered in steps of $<5 \mu\text{m}$ to isolate the complex spike activity of a Purkinje cell. The signal was fed into a window discriminator that allowed the number of complex spikes above the noise envelope to be sampled and stored in the computer. Once a unit was isolated, the rabbit was presented with either unpaired tones and airpuffs or paired tone-airpuff trials. Trials were presented until the cell was lost or enough trials were collected to characterize the cell's activity. Small marking lesions were placed at interesting recording sites or at the bottom of electrode tracts to histologically reconstruct the path of electrode penetrations. Single units were recorded from several regions within cerebellar cortex likely to be involved in eyeblink conditioning, including lobule HVI, HV (anterior lobe), HVIIA (crus I), and paramedian lobule. The following criteria were used to identify Purkinje cells: (i) the presence of both simple and complex spikes in the same unit recording; (ii) characteristic activity through different cortical layers (molecular, Purkinje cell, granule cell); and (iii) histological reconstructions—recording sites located within the Purkinje cell layer were identified by Nissl staining. Only the cells that reliably fit each of the above criteria were classified as Purkinje cells.
 17. P. Angaut and C. Sotelo, *Neurosci. Lett.* **83**, 227 (1987); A. R. Gibson, F. R. Robinson, J. Alam, J. C. Houk, *J. Comp. Neurol.* **260**, 362 (1987); G. Andersson, M. Garwicz, G. Hesslow, *Brain Res.* **472**, 450 (1988); P. Angaut and C. Sotelo, *ibid.* **479**, 361 (1989); B. J. Fredette and E. Mugnaini, *Anat. Embryol.* **184**, 225 (1991); P. Angaut, C. Compoint, C. Buisseret-Delmas, C. Batini, *Neurosci. Res.* **26**, 345 (1996).
 18. For PTX infusions ($1 \mu\text{l}$ of $10 \mu\text{M}$ at a rate of $0.1 \mu\text{l}/\text{min}$), a guide cannulae was implanted into the contralateral dorsal accessory portion of the inferior olive ($n = 2$ animals). The placement of the cannulae was aided by monitoring characteristic inferior olive cell activity (groups of two to three spikes, low spontaneous rates) with a recording electrode protruding from the cannulae. Interestingly, by removing the GABA-mediated inhibition in the inferior olive, PTX seems to increase the overall frequency of complex spike activity recorded in the cerebellum.
 19. Blocking procedures: (Phase I) Two blocking groups (ACSF and PTX) underwent 7 days of tone-airpuff conditioning. Controls were restrained in the training

apparatus for the same amount of time. All groups received intraolivary ACSF infusions on the last day. (Phase II) Animals were then subjected to 5 days of tone-light-airpuff compound conditioning. During this phase, ACSF and PTX ($1 \mu\text{M}$) were infused continuously at a rate of $0.1 \mu\text{l}/\text{min}$ from 15 min before training up to the end of training. (Test phase) Animals were given 5 days of light-airpuff savings testing. Daily training was divided into 10 blocks with each block consisting of 10 trials, totaling 100 trials. With each block, the first and sixth trials were CS-only and US-only trials, respectively, and the remainder were paired trials. The tone CS was 1 kHz, 85 dB, and a duration of 500 ms, the light CS was 45 lux and 500 ms, and the airpuff US was 2.3 N/m^2 and 100 ms. In our preparation, the external eyelids were held open and the corneal airpuff US was delivered

to the temporal region of the cornea, a region not covered by the nictitating membrane at full extension. Both CSs preceded the US by 400 ms and the stimuli coterminated.

20. A. M. Graybiel, T. Aosaki, A. W. Flaherty, M. Kimura, *Science* **265**, 1826 (1994).
21. W. Schultz, P. Apicella, T. Ljungberg, *J. Neurosci.* **13**, 900 (1993); W. Schultz, P. Dayan, P. R. Montague, *Science* **275**, 1593 (1997).
22. We thank A. R. Wagner and M. M. Chun for their helpful comments on the manuscript. Supported by grants (R.F.T.) from the U.S. National Institute on Aging (AF05142), NSF (IBN9215069), and the U.S. Office of Naval Research (N00014-95-1-1152), and also the Sankyo Corporation.

12 September 1997; accepted 2 December 1997

Role of Dynamin in the Formation of Transport Vesicles from the Trans-Golgi Network

Steven M. Jones, Kathryn E. Howell, John R. Henley, Hong Cao, Mark A. McNiven*

Dynamin guanosine triphosphatases support the scission of clathrin-coated vesicles from the plasmalemma during endocytosis. By fluorescence microscopy of cultured rat hepatocytes, a green fluorescent protein–dynamin II fusion protein localized with clathrin-coated vesicles at the Golgi complex. A cell-free assay was utilized to demonstrate the role of dynamin in vesicle formation at the trans-Golgi. Addition of peptide-specific anti-dynamin antibodies to the assay mixture inhibited both constitutive exocytic and clathrin-coated vesicle formation. Immunodepletion of dynamin proteins also inhibited vesicle formation, and budding efficiency was restored upon readdition of purified dynamin. These data suggest that dynamin participates in the formation of distinct transport vesicles from the trans-Golgi network.

The dynamins comprise a family of 100-kD guanosine triphosphatases that have been implicated in severing clathrin-coated invaginations from the plasma membrane based on the *shibire^{ts1}* mutant of *Drosophila melanogaster* (1) and studies of a mutant dynamin isoform overexpressed in mammalian epithelial cells (2–4). Originally dynamin was thought to be a neuronal specific protein. However, three distinct dynamin genes recently have been identified in mammals: dynamin I (*Dyn1*) is expressed exclusively in neurons (5, 6); dynamin II (*Dyn2*) is found in all tissues (6); and dynamin III (*Dyn3*) is restricted to the testis, the brain, and the lung (7). Each dynamin gene encodes at least four alternatively spliced isoforms (8). Whether all these dynamin gene products function solely at the plasma membrane or also mediate other vesicle scission events at distinct cellular sites is unknown (8). Recently, a dynamin

has been localized to the Golgi complex of mammalian cells by biochemical, immunological, and morphological techniques (9, 10). To provide additional evidence supporting the Golgi localization of a specific dynamin isoform, we linked Dyn2 (spliced form “aa”) to green fluorescent protein (GFP) and expressed it in a rat hepatocyte cell line. Subsequently, its distribution was followed in vivo by fluorescence microscopy (11–13) (Fig. 1). In parallel, untransfected cells were labeled with a Dyn2-specific antibody and a Pan-dynamin antibody (MC63), which recognizes a conserved region of the dynamins (14). A prominent punctate staining at the plasma membrane and the Golgi region was observed with both experimental protocols [GFP-Dyn2 in vivo (Fig. 1, B and D) and endogenous Dyn2 after fixation and immunolocalization (Fig. 1, A, B', C, and D')]. Thus, the transfection process did not alter the distribution of the endogenous Dyn2 compared with untransfected cells. Importantly, the overlap between the two images (Fig. 1) suggests that a Dyn2 isoform is localized to vesicles at both the plasma membrane and the Golgi complex.

To define more precisely the localization of Dyn2 at the Golgi region, cells expressing

J. R. Henley, H. Cao, M. A. McNiven, Center for Basic Research in Digestive Diseases, Mayo Clinic and Foundation, Rochester, MN 55905, USA.

S. M. Jones, K. E. Howell, Department of Cellular & Structural Biology, University of Colorado School of Medicine, 4200 East 9th Avenue, Denver, CO 80262, USA.

*To whom correspondence should be addressed. E-mail: mcniven.mark@mayo.edu

GFP-Dyn2 were labeled with antibodies to either clathrin or an antigen of the trans-Golgi, TGN38 (14). A nearly identical fluorescence pattern was observed between GFP-Dyn2 and the clathrin labeling (Fig. 2, A to A''). The significant overlap between GFP-Dyn2 and clathrin at the Golgi region suggests that Dyn2 may associate with nascent clathrin-coated buds forming at the trans-Golgi network (TGN). These images also demonstrate a colocalization of GFP-Dyn2 and clathrin at the plasma membrane and provide an important control, as others have shown a colocalization of dynamin and clathrin by double labeling and conventional immunofluorescence microscopy (3, 15). The localizations of TGN38 and GFP-Dyn2 were nearly identical in the central region of the cells; however, the overlap on peripheral vesicles was significantly less than with clathrin (Fig. 2, B to B''). Thus, at least one spliced variant of dynamin (Dyn2aa) associates with clathrin-coated vesicles at the TGN in these cells and probably is more widely distributed than the clathrin-coated vesicles in the TGN. A similar distribution was observed in cells that expressed the spliced variant Dyn2ba (16). Therefore, Dyn2 may function in vesicle budding events at the TGN.

To support the morphological localization of Dyn2 at the Golgi complex, we conducted complementary biochemical studies. We determined the amount of dynamin binding to a highly enriched rat liver Golgi fraction (17) under three conditions, all containing added cytosol (100,000g liver supernatant): alone in the absence of adenosine triphosphate (ATP), with added ATP, and with an ATP regeneration system either without or with guanosine 5'-O-(2-thiodiphosphate) (GTP- γ -S) (18). After the incubation, Golgi fractions were sepa-

rated from cytosol and subjected to SDS-polyacrylamide gel electrophoresis (SDS-PAGE) and immunoblot analysis with the Pan-dynamin antibody MC63. When dynamin was incubated with cytosol alone, a

minimal amount of it was found associated with the Golgi fraction (Fig. 3A). When ATP and an ATP regeneration system were added to the incubation mixture, a 3-fold increase in dynamin binding was observed

Fig. 2. GFP-Dyn2 associates with clathrin-coated vesicles at both the plasma membrane and the TGN. Double-label fluorescence microscopy of clone 9 cells expressing GFP-Dyn2. (A and B) GFP-Dyn2 is localized to punctate vesicles at the plasma membrane and in the Golgi region. Immunolocalization of the same cell with a monoclonal clathrin antibody (A') shows a nearly identical localization with the GFP-Dyn2 at the plasma membrane and the Golgi complex. Immunolocalization with an antibody to TGN38 (B') shows a nearly identical localization of the GFP-Dyn2 with the prominently labeled Golgi. Bars = 10 μ m.

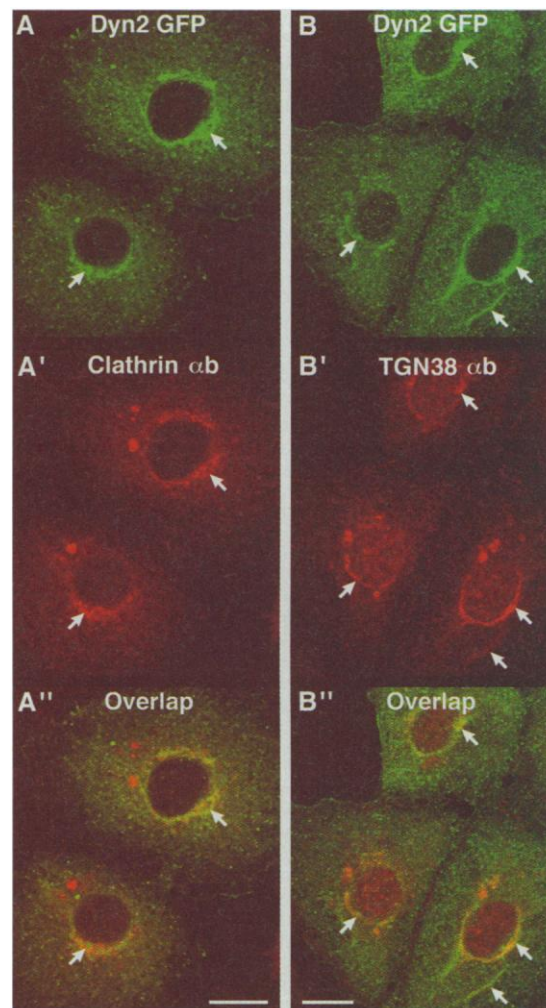
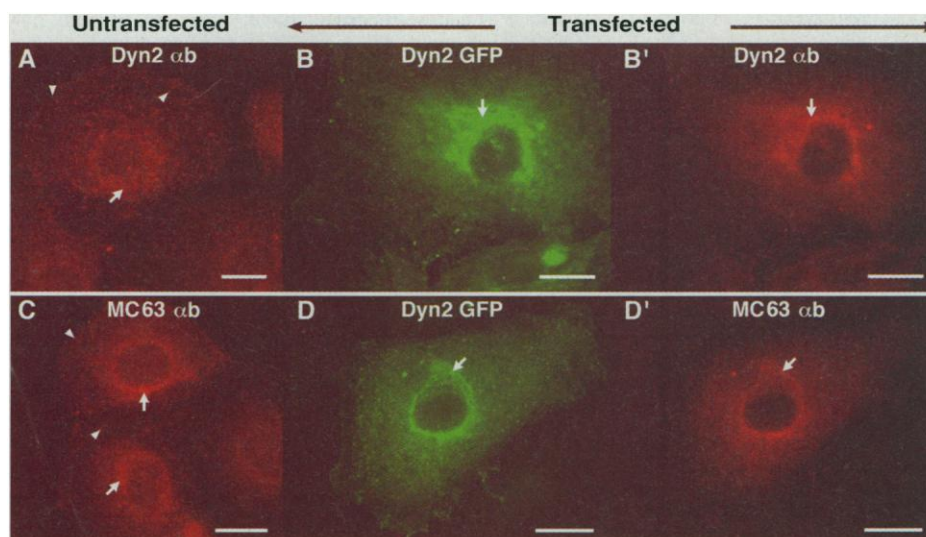


Fig. 1. A GFP-Dyn2 protein expressed in cultured hepatocytes localizes to the plasma membrane and perinuclear vesicles. (A and C) Immunofluorescence microscopy of nontransfected clone 9 cells stained with affinity-purified antibodies specific for Dyn2 (A) or the Pan-dynamin antibody MC63 (C), which recognizes all dynamin isoforms [for details of antibodies see (14)]. Numerous punctate vesicles are seen at the cell periphery near the plasma membrane (arrowheads) and around the nucleus (arrows). (B and D) Clone 9 cells transfected with a GFP-Dyn2 construct and viewed in vivo with a cooled CCD video camera. The GFP-Dyn2 localizes to vesicles at the plasma membrane and in the Golgi region, a pattern similar to the localization obtained with antibodies against dynamin in untransfected cells (A and C). (B' and D') The GFP-Dyn2-expressing cells stained with the Dyn2-specific (B') or MC63 (D') antibodies show colocalization of overexpressed and endogenous forms of dynamin. Bars = 10 μ m.



and the addition of GTP- γ -S resulted in a 10-fold increase in dynamin binding. These experiments support the morphological observations that dynamin associates with the Golgi and demonstrate that this association is energy-dependent.

To test whether Dyn2 acts in vesicle formation from the TGN as it does at the plasma membrane, we used a cell-free assay of vesicle formation from the TGN (19, 20). This assay measures the formation of both polymeric immunoglobulin A receptor (pIgA-R)-containing (constitutive) exocytic vesicles and clathrin-coated vesicles from the TGN by using a purified rat liver stacked Golgi fraction. Consistent with previous work (19), in the complete system the budding efficiency of the mature form of the pIgA-R was ~70%, and in the absence of cytosol had a background of less than 5% (Fig. 4C). In the absence of cytosol, the background of clathrin-coated vesicle budding also was less than 5% (Fig. 4D). First, the effect of dynamin antibodies on vesicle formation was tested. Three different affinity-purified peptide antibodies against conserved or isoform-specific domains of the dynamins (Fig. 3B) [see (14) for discussion of antibody specificity] were added to the assay mixture in increasing concentrations (0 to 16 μ g). Antibodies against a conserved region of the kinesin heavy chain (MC44) or vesicular stomatitis virus G protein (P5D4) (17) were used at the same concentrations and served as controls. Although control antibodies did not inhibit the budding of

pIgA-R-containing or clathrin-coated vesicles at any of the concentrations tested, the formation of both vesicle populations was inhibited significantly by the MC63 and Dyn2-specific antibodies (Fig. 3B). Inhibition with MC63 was apparent with 1 to 2 μ g of antibody and nearly complete inhibition was achieved with ~8 μ g of antibody. The Dyn2-specific antibody was slightly less efficient at inhibiting the formation of both vesicle populations and the MC60 antibody only partially inhibited vesicle budding. The MC63 and Dyn2-specific antibodies showed the highest immunoreactivities by immunoblot analysis and immunofluorescence microscopy (21), which may explain the differences observed between antibodies in these functional inhibition studies. MC63 specifically labels the Golgi by immunofluorescence microscopy and efficiently immunoprecipitates Golgi components (9). Because antibodies against two distinct dynamin domains effectively inhibited the formation of both vesicle populations, whereas control antibodies had no effect, these reagents demonstrate a specific block of dynamin function at the TGN.

To provide an additional test for the participation of dynamin in vesicle formation from the TGN, the cell-free assay was carried out either with cytosol immunodepleted of dynamin proteins or after readdition of a dynamin-enriched preparation to the depleted cytosol (Fig. 4). Dynamin was depleted from rat liver cytosol by using two immunoaffinity columns made from the MC63 and

Dyn2-specific antibodies (22). By SDS-PAGE and Coomassie blue staining, we found that the starting rat liver cytosol and depleted cytosol did not differ significantly (Fig. 4A). In contrast, immunoblot analyses of these fractions clearly showed a complete depletion of dynamin from the cytosol (Fig. 4A). For reconstitution of the depleted cytosol, a dynamin-enriched fraction was prepared from rat brain by column chromatography (23) (Fig. 4B). This purification procedure was utilized because the conditions used to elute dynamin proteins from the immunoaffinity column inactivated the protein. Standard chromatographic methods provided a highly enriched dynamin preparation that contained all three dynamin isoforms (Dyn1, -2, and -3). Significantly, depletion of dynamin proteins from the cytosol totally inhibited both exocytic and clathrin-coated vesicle formation (Fig. 4, C and D). Readdition of the dynamin-enriched fraction to the depleted cytosol restored the budding activity of both vesicle populations in a concentration-dependent manner, with ~25 μ g sufficient to restore budding to near control levels. Addition of 50 μ g of the enriched dynamin fraction alone (without the depleted cytosol) could not restore any budding activity, which supports the observations indicating that other cytosolic components are required for budding (24).

The immunolocalization studies (9, 10) combined with the GFP-Dyn2 localization and the functional experiments presented here demonstrate a requirement for dynamin

Fig. 3. Antibodies to dynamin inhibit vesicle formation from the Golgi complex. (A) Dynamin binding to a highly enriched Golgi fraction. The SGF1 was incubated with a cytosolic fraction in the absence of ATP (lane 1); in the presence of ATP and an ATP-regenerating system (lane 2); or in the presence of ATP, an ATP-regenerating system, and 10 μ M GTP- γ -S (lane 3) at 37°C for 15 min. The reaction mixture was centrifuged through a sucrose cushion and the Golgi pellet was immunoblotted and analyzed for the presence of dynamin. The dynamin-immunoreactive band at 100 kD is shown in the upper panel, and quantitation of the amount of dynamin bound (PhosphorImager units) is shown in the lower panel. Note the increase in the association of dynamin with the Golgi membranes in the presence of either ATP or GTP- γ -S. Each assay was carried out in triplicate and the standard error is plotted. (B) Antibodies to dynamin inhibit formation of both the pIgA-R-containing exocytic and clathrin-coated vesicles. (Top) Domains of Dyn2 are diagrammed and include three GTP-binding consensus sequence elements in the NH₂-terminus, a pleckstrin homology (PH) domain in the COOH-terminal region, and a proline-rich domain at the COOH-terminus. The regions used to generate the polyclonal MC60, MC63, and Dyn2-specific antibodies are noted. The MC60 and MC63 epitopes are present in all dynamin isoforms, whereas the Dyn2-specific epitope is unique to Dyn2. (Middle and bottom) Cell-free assays of vesicle budding from the TGN were carried out in the presence of increasing amounts (0 to 16 μ g) of affinity-purified antibodies. The budding efficiencies of the pIgA-R-containing vesicles (middle) and clathrin-coated vesicles (bottom) are plotted against

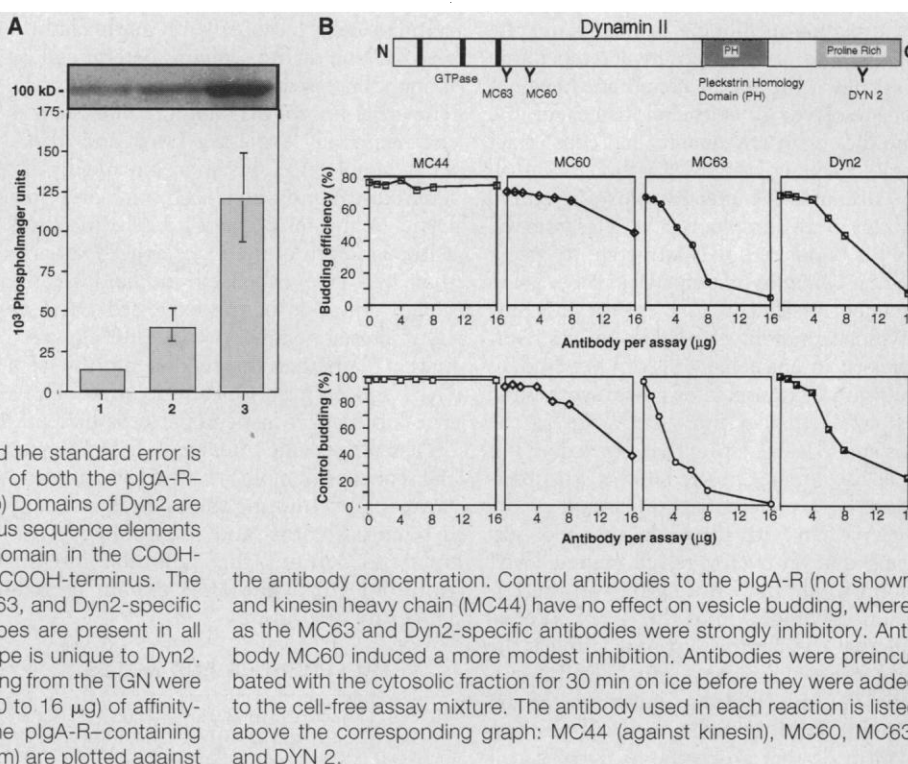
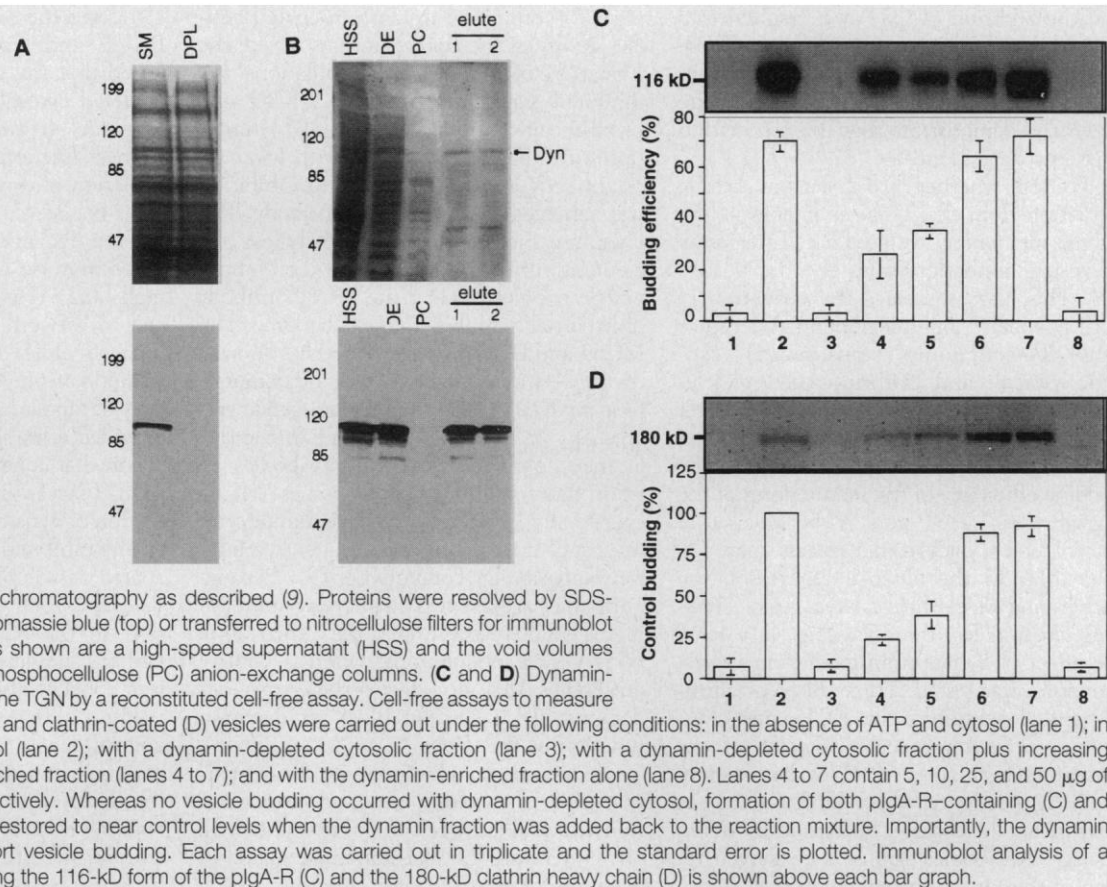


Fig. 4. Vesicle formation from the TGN is dependent on dynamin and cytosolic factors. **(A)** Immunodepletion of dynamin from rat liver cytosol using immunoaffinity columns. A rat liver cytosolic fraction was passed over two successive antibody columns and the nonbound fractions were collected and concentrated. Fractions of the starting (SM) and immunodepleted (DPL) cytosolic fraction were resolved by SDS-PAGE and stained with Coomassie blue (top) or transferred to nitrocellulose filters and blotted with the Pan-dynamin antibody MC63 (bottom). **(B)** Generation of an enriched dynamin fraction from rat brain for use in restoration experiments. A rat brain dynamin-enriched fraction (elute) was obtained by ion-exchange column chromatography as described (9). Proteins were resolved by SDS-PAGE and either stained with Coomassie blue (top) or transferred to nitrocellulose filters for immunoblot analysis (bottom). Other fractions shown are a high-speed supernatant (HSS) and the void volumes collected from DEAE (DE) and phosphocellulose (PC) anion-exchange columns. **(C and D)** Dynamin-dependent vesicle budding from the TGN by a reconstituted cell-free assay. Cell-free assays to measure budding of plgA-R-containing (C) and clathrin-coated (D) vesicles were carried out under the following conditions: in the absence of ATP and cytosol (lane 1); in the presence of ATP and cytosol (lane 2); with a dynamin-depleted cytosolic fraction (lane 3); with a dynamin-depleted cytosolic fraction plus increasing concentrations of a dynamin-enriched fraction (lanes 4 to 7); and with the dynamin-enriched fraction alone (lane 8). Lanes 4 to 7 contain 5, 10, 25, and 50 μ g of dynamin-enriched fraction, respectively. Whereas no vesicle budding occurred with dynamin-depleted cytosol, formation of both plgA-R-containing (C) and clathrin-coated (D) vesicles was restored to near control levels when the dynamin fraction was added back to the reaction mixture. Importantly, the dynamin preparation alone did not support vesicle budding. Each assay was carried out in triplicate and the standard error is plotted. Immunoblot analysis of a representative experiment showing the 116-kD form of the plgA-R (C) and the 180-kD clathrin heavy chain (D) is shown above each bar graph.



proteins in the formation of two different vesicle populations from the TGN. Although dynamin rings around the necks of forming TGN vesicles have not been reported, these structures have been observed only at the plasma membrane in neurons of the *shibire^{ts1}* flies at the restrictive temperature (8). Rings at the plasma membrane have not been resolved in epithelial tissues of the same flies or in any mammalian cells under physiological conditions (without GTP- γ -S). Although the precise role of dynamin isoforms in the formation of vesicles from the TGN is undefined, it is attractive to speculate that dynamin participates in the scission of nascent vesicles (9, 25). A previous study in which a mutant Dyn1 protein was overexpressed in epithelial cells did not find an inhibition of transport of newly synthesized hydrolytic enzymes from the Golgi to the lysosome (3), suggesting that Dyn1 does not act at the TGN. On the basis of our observations of a preferential association of the Dyn2 protein with the Golgi, it is not surprising that an overexpressed mutant Dyn1 isoform would have little effect on the formation of vesicles from the TGN. We assume that Dyn2 is the dynamin acting at the TGN for several reasons. First, Dyn2 is currently the only dynamin known to be expressed in most epithelial cells (6). Second, an antibody that is specific for Dyn2 local-

ized this isoform to the Golgi complex by immunofluorescence microscopy (Fig. 1) and inhibited vesicle formation from the TGN in the cell-free assay (Fig. 3, C and D). Finally, a GFP-Dyn2 protein expressed in cultured cells localized with both clathrin and TGN38 at the Golgi as determined by immunofluorescence microscopy (Fig. 2). The other known dynamin proteins, such as the neuronally expressed Dyn1 and Dyn3, when coupled to GFP, show a markedly different distribution from each other and from Dyn2 in the rat hepatocyte cell line (26). Although both of the Dyn2 spliced variants that we have expressed localized to the Golgi, only one of the expressed Dyn1 or Dyn3 proteins showed a modest Golgi association. Whether the modest affinity of a Dyn1 spliced form for the Golgi reveals its true localization in neuronal cells or represents a nonspecific interaction based on partial sequence homology to the Dyn2 forms is unclear. Determining the roles of the many dynamin isoforms and their spliced variants and defining the molecular interactions of Dyn2 at the TGN remain as challenges for the future.

REFERENCES AND NOTES

1. T. A. Grigliatti, L. Hall, R. Rosenbluth, D. T. Suzuki, *Mol. Gen. Genet.* **120**, 107 (1973); T. Kosaka and K. Ikeda, *J. Neurobiol.* **14**, 207 (1983); *J. Cell Biol.* **97**,

- 499 (1983); J. H. Koenig and K. Ikeda, *J. Neurosci.* **9**, 3844 (1989); C. A. Poodry, *Dev. Biol.* **138**, 464 (1990); M. S. Chen *et al.*, *Nature* **351**, 583 (1991); A. M. van der Bliek and E. M. Meyerowitz, *ibid.*, p. 411.
2. J. S. Herskovits, C. C. Burgess, R. A. Obar, R. B. Vallee, *J. Cell Biol.* **122**, 565 (1993); A. M. van der Bliek *et al.*, *ibid.*, p. 553.
3. H. Damke, T. Baba, D. E. Warnock, S. L. Schmid, *ibid.* **127**, 915 (1994).
4. H. Damke, T. Baba, A. M. van der Bliek, S. L. Schmid, *ibid.* **131**, 69 (1995).
5. R. A. Obar, C. A. Collins, J. A. Hammarback, H. S. Shpetner, R. B. Vallee, *Nature* **347**, 256 (1990).
6. T. A. Cook, R. Urrutia, M. A. McNiven, *Proc. Natl. Acad. Sci. U.S.A.* **91**, 644 (1994); J. M. Sontag *et al.*, *J. Biol. Chem.* **269**, 4547 (1994).
7. T. Nakata, R. Takemura, N. Hirokawa, *J. Cell Sci.* **105**, 1 (1993); T. Cook, K. Mesa, R. Urrutia, *J. Neurochem.* **67**, 927 (1996).
8. R. Urrutia, J. R. Henley, T. Cook, M. A. McNiven, *Proc. Natl. Acad. Sci. U.S.A.* **94**, 377 (1997).
9. J. R. Henley and M. A. McNiven, *J. Cell Biol.* **133**, 761 (1996).
10. O. Maier, M. Knoblich, P. Westermann, *Biochem. Biophys. Res. Commun.* **223**, 229 (1996).
11. For overexpression of Dyn2, the full-length sequence of Dyn2aa was amplified by polymerase chain reaction (PCR) from rat brain cDNA using primers H-N5' (5'-aagcttGGACCATGGGCAACCGGGATGG-AAGAG) and H-N3' (5'-gaattccCCCAGAACACTGTCCCCTGCAGCGTGA). A PCR fragment was cloned into the Hind III and Eco RI sites of the mammalian expression vector pEGFP N1 (Clontech, Palo Alto, CA) under control of the cytomegalovirus promoter. Clone 9 cells, a normal rat hepatocyte cell line [CRL-1439, American Type Culture Collection (ATCC), Rockville, MD], were electroporated (3×10^6 cells per milliliter) with purified Dyn2 DNA (50 μ g of DNA) (cuvette gap, 0.4 cm; voltage, 0.3 kV; capacitance, 250 μ F) using a Bio-Rad instrument (Her-

- cules, CA). After 24 hours, selection was initiated by addition of G418 (400 $\mu\text{g}/\text{ml}$) to the cell culture medium. A stable clone 9 cell line overexpressing GFP-Dyn2 was achieved within a month.
12. Clone 9 cells were maintained at 37°C in Ham's F-12K medium supplemented with 10% fetal bovine serum. Cells were grown on cover glasses for 1 to 3 days before microscopy.
 13. For immunolocalization, cells were fixed in aldehyde and then labeled as described (9) and mounted in ProLong antifade reagent (Molecular Probes, Eugene, OR). Alternatively, live cells were viewed directly. Either an epifluorescence microscope (Axiovert 35, Carl Zeiss) equipped with a 100-W mercury arc (attenuated up to 90%) and a cooled charged coupled device (CCD) camera (SenSys, Photometrics, Tucson, AR) or a confocal laser scanning microscope (LSM-410, Carl Zeiss) was used for fluorescence microscopy.
 14. The location of each peptide used as antigen within the dynamin molecule is shown in Fig. 3B. The Pan-dynamin MC63 antibody has been shown to specifically recognize a 100-kD dynamin band in rat liver fractions by immunoblotting and immunoprecipitation (9). The Pan-dynamin MC60 and Dyn2-specific antibodies also have been characterized (27). The antibodies added to cell-free assays were affinity purified and concentrated (~3 mg/ml); then they were tested by immunoblot analysis to confirm retention of activity (9). Antiserum against clathrin was produced from the hybridoma X22 (ATCC). The antibodies against the cytoplasmic and luminal domains of the plgA-R have been described (19). The rabbit polyclonal antibody to TGN38 was to a peptide representing the COOH-terminal cytoplasmic portion of the protein.
 15. K. Takei, P. S. McPherson, S. L. Schmid, P. De Camilli, *Nature* **374**, 186 (1995).
 16. S. M. Jones, K. E. Howell, J. R. Henley, H. Cao, M. A. McNiven, data not shown.
 17. R. S. Taylor, S. M. Jones, R. H. Dahl, M. H. Nordeen, K. E. Howell, *Mol. Biol. Cell* **8**, 1911 (1997).
 18. For the membrane binding assay, stacked Golgi fractions (SGF1) were isolated from rat liver (17). SGF1 (100 μg) plus cytosol (200 μg) were incubated in 25 mM Hepes (pH 6.7), 25 mM KCl, 1.5 mM magnesium acetate in a final volume of 1.0 ml at 37°C for 15 min. For assay mixtures that contained ATP, 1.0 mM ATP and an ATP regenerating system (8.0 mM creatine phosphate, 0.043 mg of creatine phosphokinase per milliliter) were added to the reaction mixture. For other assays GTP- γ -S was added to a final concentration of 10.0 μM . After incubation, the reaction mixture was loaded onto a 0.5 M sucrose cushion and centrifuged in a TLS55 rotor at 55,000 rpm for 1 hour. Membrane pellets were resolved by SDS-PAGE, transferred to nitrocellulose filters, immunoblotted with antibodies against dynamin (MC63), which were detected with ¹²⁵I-labeled protein A (NEN, Boston, MA), and exposed to film for autoradiography. Immunoblots were quantitated with a PhosphorImager (Molecular Dynamics, Sunnyvale, CA).
 19. J. Salameo, E. S. Sztul, K. E. Howell, *Proc. Natl. Acad. Sci. U.S.A.* **87**, 7717 (1990).
 20. The cell-free assay of budding from immobilized stacked Golgi fractions was carried out as described (24). Each assay mixture contained a 2.5-mg magnetic core and shell beads with ~50 μg of the stacked Golgi fraction immobilized. The immobilized fraction has been characterized (24). For the budding reaction, the immobilized fraction was incubated in 2.5 ml containing cytosol at 0.70 mg/ml, 25 mM Hepes (pH 6.7), 25 mM KCl, 1.5 mM magnesium acetate, 1.0 mM ATP, an ATP regenerating system (8.0 mM creatine phosphate, 0.043 mg of creatine phosphokinase per milliliter), and 5 mg of bovine serum albumin (BSA) per milliliter (final concentrations). For cell-free assays in which antibodies were tested, increasing concentrations of antibody were incubated with the cytosol for 30 min on ice before addition to the cell-free assay. After 10 min at 37°C the Golgi fraction remaining on the beads was retrieved, and the budded vesicles remained in the supernatant. The budded fraction was pelleted through a 0.25 M sucrose cushion (100,000g for 1 hour) to deplete the BSA (5 mg/ml) and large amounts of cytosolic proteins. The pellet was resuspended in gel sample buffer and resolved by SDS-PAGE. Budding efficiency was reported as the percentage of the total mature sialylated plgA-R (116 kD) present in the budded fraction (100% represents the amount present in the immobilized SGF before budding). The plgA-R distribution was determined by quantitative immunoblotting of the fractions from the cell-free assay. Because the plgA-R is a plasma membrane receptor synthesized in relatively high amounts in rat liver (28), it defines a specific population of constitutive exocytic vesicles (24). The amount of clathrin-coated vesicle formation was assessed by determining the amount of clathrin heavy chain in the total budded vesicle fraction by quantitative immunoblotting with monoclonal antibody TD.1 (ATCC). Percentage budding was calculated as the amount of clathrin heavy chain in the pelleted total budded fraction compared with that found in control budding reactions (100%). The amount of clathrin-coated vesicle budding in the absence of ATP and cytosol was 3%.
 21. S. M. Jones, K. E. Howell, J. R. Henley, H. Cao, M. A. McNiven, data not shown.
 22. For depletion of dynamin proteins from rat liver cytosol, 2 ml of rat liver cytosol (16 mg/ml), prepared by the methods of Palade and coworkers (28), was passed repeatedly over an MC63 Pan-dynamin antibody column at 4°C. The cytosolic void volume next was passed repeatedly over a Dyn2-specific antibody column at 4°C. The void volume was concentrated, separated by SDS-PAGE, and immunoblotted with dynamin antibodies to confirm a complete depletion of dynamin proteins from the cytosol. The dynamin antibody columns were prepared by immobilizing 9.3 mg and 4.9 mg of affinity-purified MC63 or Dyn2-specific antibodies, respectively, per 1.5-ml column matrix. All antibodies were immobilized by using an Immunopure protein A IgG orientation kit (Pierce Chemical, Rockford, IL) according to the manufacturer's instructions.
 23. A dynamin-enriched fraction was isolated from freshly obtained rat brains according to established methods (9, 29). Briefly, a rat brain homogenate was passed through a 10-ml DEAE anion-exchange column and then added to a 5-ml phosphocellulose column. After substantial rinsing in 100 mM NaCl buffer, dynamin proteins were eluted from the column with 250 mM NaCl, and then the fractions were pooled, concentrated, dialyzed, and frozen in liquid nitrogen.
 24. S. M. Jones, R. H. Dahl, J. Ugelstad, K. E. Howell, in *Cell Biology: A Laboratory Handbook*, J. E. Celis, Ed. (Academic Press, London, ed. 2, 1997), vol. 2, pp. 12-25; M. Jones and K. E. Howell, *J. Cell Biol.* **139**, 339 (1997).
 25. R. B. Kelly, *Nature* **374**, 116 (1995); J. Roos and R. B. Kelly, *Trends Cell Biol.* **7**, 257 (1997).
 26. H. Cao and M. A. McNiven, unpublished work.
 27. J. R. Henley, E. W. A. Krueger, B. J. Oswald, M. A. McNiven, *J. Cell Biol.*, in press.
 28. E. S. Sztul, K. E. Howell, G. E. Palade, *ibid.* **100**, 1255 (1985).
 29. R. Scaife, I. Gout, M. D. Waterfield, R. L. Margolis, *EMBO J.* **13**, 2574 (1994).
 30. At UCHSC the use of the Hepatobiliary Center, Cell Biology Core (NIH, P30 DK-34914), and the Cancer Center Monoclonal Antibody Facility (P30 CA-46934) is acknowledged. We especially thank J. Ugelstad and R. Schmid, SINTEF, University of Trondheim, Norway, for the shell and core magnetic beads used in the cell-free assay. Thanks also goes to F. Garcia for her help with the GFP expression studies, to E. Krueger for his work on the GFP imaging, and to B. Oswald for help with preparation of antibodies and depleted cytosol.

12 September 1997; accepted 9 December 1997

Gain-of-Function Mutations of *c-kit* in Human Gastrointestinal Stromal Tumors

Seiichi Hirota,* Koji Isozaki,* Yasuhiro Moriyama, Koji Hashimoto, Toshirou Nishida, Shingo Ishiguro, Kiyoshi Kawano, Masato Hanada, Akihiko Kurata, Masashi Takeda, Ghulam Muhammad Tunio, Yuji Matsuzawa, Yuzuru Kanakura, Yasuhisa Shinomura, Yukihiko Kitamura†

Gastrointestinal stromal tumors (GISTs) are the most common mesenchymal tumors in the human digestive tract, but their molecular etiology and cellular origin are unknown. Sequencing of *c-kit* complementary DNA, which encodes a proto-oncogenic receptor tyrosine kinase (KIT), from five GISTs revealed mutations in the region between the transmembrane and tyrosine kinase domains. All of the corresponding mutant KIT proteins were constitutively activated without the KIT ligand, stem cell factor (SCF). Stable transfection of the mutant *c-kit* complementary DNAs induced malignant transformation of Ba/F3 murine lymphoid cells, suggesting that the mutations contribute to tumor development. GISTs may originate from the interstitial cells of Cajal (ICCs) because the development of ICCs is dependent on the SCF-KIT interaction and because, like GISTs, these cells express both KIT and CD34.

The *c-kit* proto-oncogene encodes a type III receptor tyrosine kinase (KIT) (1), the ligand of which is SCF (2). SCF-KIT interaction is essential for development of melanocytes, erythrocytes, germ cells, mast cells and ICCs (3, 4). Gain-of-function mu-

tations of the *c-kit* gene have been found in several tumor mast cell lines of rodents and humans (5, 6) and in mast cell tumors of humans (7). Here we investigate the mutational status of *c-kit* in mesenchymal tumors of the human gastrointestinal (GI) tract.